Turkish Journal of Electrical Engineering & Computer Sciences

http://journals.tubitak.gov.tr/elektrik/

Research Article

Turk J Elec Eng & Comp Sci
(2016) 24: 4885 – 4899

doi:10.3906/elk-1502-167

Solar irradiation estimator based on a self-calibrated reference solar cell

Touria HASSBOUN*, Lhoussain EL BAHIR, Youness AITE DRISS, Mustapha EL ADNANI

Laboratory of Electrical Engineering and Control Systems (LGECOS), National School of Applied Sciences, Cadi Ayyad University, Marrakech, Morocco

Received: 19.02.2015 • **Accepted/Published Online:** 24.09.2015 • **Final Version:** 06.12.2016

Abstract: In this paper we propose a concept for estimating solar irradiation based on measurements of the current, voltage, and temperature of a photovoltaic (PV) cell.

The estimation of the irradiation is obtained by processing these measurements using a PV cell mathematical model combined with a PI controller. Since the PV cell current is very sensitive to the irradiance level, the principle of the method is to force the model to reproduce the same current as that measured on the cell by applying an appropriate irradiance as input, for measured temperature and voltage. The appropriate irradiance, which is the output of our estimator, is provided by the PI controller in such way that the current estimated by the model follows exactly the measured current. The PI controller ensures also self-calibration of the PV reference cell depending on the temperature changes. The effectiveness of the proposed approach has been validated in a simulation and implemented in real time using the dSpace 1104 board.

Key words: Photovoltaic, solar energy, solar cell, solar irradiation, solar cell calibration, renewable energy

1. Introduction

In recent decades, green energy sources including solar energy have attracted interest for power generation and transmission systems. Being an inexhaustible and renewable source of energy and due to the nature of solar radiation energy conversion to electricity, photovoltaic energy has particularly been adopted as a potential alternative source in many fields, such as aerospace industries, electrical vehicles, communication equipment, and grid connected PV systems [1–3].

Solar energy uses photovoltaic (PV) modules to convert sunlight into electricity. Moreover, the performance of these PV modules is strongly dependent on the solar irradiance, ambient temperature, and module temperature [4,5]. Solar radiation represents the sunlight intensity, which has a practically proportional relationship with the output current from the PV module. High radiation intensity induces a high output PV current and then a higher PV power [6,7].

In PV systems, it is necessary to use optimization techniques to work around the optimum operating point [8,9]. Solar irradiation magnitude is a significant factor that influences the behavior of the I–V (current–voltage) characteristic of the PV module. It is a key parameter of the performance of the PV generator and its efficiency depends strongly on the spectral distribution of the insolation [5].

PV devices are generally evaluated according to a standard spectral distribution as a reference. Datasheets

*Correspondence: t.hassboun@uca.ma

generally give information about the characteristics and performance of PV devices with respect to the so-called standard test condition (STC), which means an irradiation of 1000 W/m^2 with an AM1.5 spectrum at 25 ° C. The direct-normal and global AM1.5 are defined as standard terrestrial spectral distributions and are used as standards in the PV industry [10,11]. The PV devices' parameters are obtained at this reference value of irradiation and a nominal temperature of 25 ° C [12,13]. Solar irradiation measurements are often available from meteorological sources. For many purposes, it is necessary to be able to know them in real time for a given location.

Many methods are proposed in the literature to estimate the behavior of climate parameters, such as solar radiation and ambient temperature. Since solar radiation correlates with the duration of sunshine, many researchers, starting with Angstrom [14], have suggested a linear relationship between the duration of sunshine and the global solar radiation. This relationship was frequently used as a standard way to estimate the global radiation from a local measurement with sufficient sunshine duration. Other researchers [15–20] have considered other additional meteorological factors in the previous linear equation to increase precision in the estimated coefficients.

In the literature, many studies have focused on techniques to determine solar irradiation values. Knowing the values of solar radiation is crucial in many application areas, namely meteorology and solar systems. Some authors are interested in local solar irradiation estimation. The relationship between solar irradiation and output voltage of a PV module by using the modeling equation and suitable experimental setup, namely a data acquisition system and two axis accelerometer, is established in [21]. The obtained relationship was used to determine the level of solar irradiation. This method depends on the PV device parameters, weather conditions, and optimization of the experimental setup. Reference [22] has proposed an algorithm for estimating effective solar irradiation using an unscented Kalman filter in a parabolic-trough field. Another method to estimate an irradiation level scheme for the maximum power point tracking (MPPT) control of PV systems based on the support-vector-regression (SVR) theory was proposed in [23]. In the two previously mentioned works, the implementation needs substantial memory and calculation time. Other studies are focused on tools for solar irradiation measures for evaluating the performance of PV generators. Pyranometers and calibrated PV reference devices (PVRDs) are the two most popular tools used by the PV industry for measuring irradiance [24,25]. According to [26–28] and the norm lEC 60904-3, to measure solar irradiance in PV applications, it would be beneficial to use the PV reference devices in terms of irradiance uncertainty estimation. The efficiency of photon-to-electron conversion is a wavelength-dependent function that is specific to various PV device technologies [26]. In practice, it is difficult to distinguish between three major factors that influence the measurements of the intensity of solar radiation. There are correlations between the solar radiation's incidence angle, the spectral content of solar radiation, and the room temperature.

In this paper, we propose a novel method to estimate the local solar irradiation intensity, based on a mathematical model of a PV cell combined with a PI controller. The latter computes an estimation of the actual irradiation value while ensuring self-calibration of the PV reference cell depending on the temperature changes.

The effectiveness of the proposed approach has been validated with MATLAB/Simulink software and implemented in real time using an SR-20 PV module, as PV reference device, and the dSpace 1104 board for data acquisition.

This paper is organized as follows. The model of the PV cells is presented in Section 2. Section 3 describes the principle of the proposed approach and presents the simulation results. Real-time implementation

results are presented in Section 4. Section 5 is dedicated to error analysis. Finally, some concluding remarks and perspectives are presented in the last section.

2. Mathematical model of the PV cell

2.1. Global principle

A PV cell is an electric power generator. Under illumination, it converts absorbed photon energy into electrical energy. Depending on the load to which it is connected, the cell can behave as a current generator or a voltage generator. A PV system naturally exhibits nonlinear $I--V$ characteristics, depending upon the solar irradiation and cell temperature [29–31].

The single diode model with the equivalent circuit, shown in Figure 1, is a simple model that is commonly used because of its practical convenience and the fact that it represents a reasonable compromise between accuracy and simplicity [12,32]. The circuit comprises a current source in parallel with a diode and a shunt resistor R_p, materializing the leakage current at the junction, and a resistivity grids resistor R_s [33,34]. I_{ph} is the current generated by the incident light and is directly proportional to the sun irradiation, $I_{0\,,cell}$ is the reverse saturation or leakage current of the diode, and I_D is the Shockley diode current.

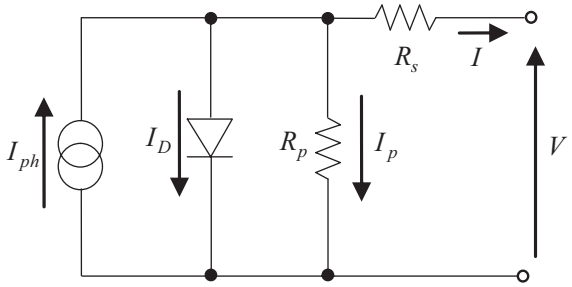

Figure 1. Equivalent circuit model of the ideal PV cell.

Based on the circuit in Figure 1, the mathematical model of a PV cell can be defined in accordance with Eqs. (1) and (2) below,

$$I = I_{ph} - I_D - I_p \text{ with } I_D = I_{0,cell}(e^{\frac{V}{AV_t}} - 1) and I_p = \frac{V + R_s I}{R_p} \tag{1}$$

$V_t = kT_c/q$ is the junction thermal voltage, q is the electron charge, k is the Boltzmann constant, T_c is the temperature of the $p--n$ junction, and A is the diode ideality constant.

The relationship between I and V is given by

$$I = I_{ph} - I_{0,cell}(e^{\frac{V+R_s I}{V_t A}} - 1) - \frac{V + R_s I}{R_p} \tag{2}$$

The current I_{ph} describes the spectrum of the PV cell and depends on climatic conditions such as ambient temperature and irradiation G as follows:

$$I_{ph} = \frac{G}{G_n}\left[I_{scr} - K_i\left(T_c - T_r\right)\right] \tag{3}$$

T_r is the reference temperature, T_c is the actual temperature of the panel, I_{scr} is the cell's short circuit current at T_r, K_i is the temperature coefficient of the short circuit, and G_n is the nominal irradiation.

The diode saturation current $I_{0,cell}$ depending on temperature may be expressed by Eq. (4) [35–37].

$$I_{0,cell} = I_{0,n}\left(\frac{T_c}{T_r}\right)^3 e^{\frac{qE_g}{Ak}\left(\frac{1}{T_r}-\frac{1}{T_c}\right)}, \tag{4}$$

where $I_{o,n}$ is the nominal saturation current and E_g is the band gap energy.

A practical PV array is composed of several connected cells. The configuration of the PV array model requires knowledge of the physical parameters of the panel, which are always provided with reference to the nominal conditions or at standard test conditions (STCs) of temperature and solar irradiation. The most important parameters widely used for describing the cell's electrical performance are the open-circuit voltage V_{oc}, the short-circuit current I_{scr}, the voltage at the maximum power point (MPP) (V_{mp}), the current at the MPP (I_{mp}), and the maximum experimental peak output power ($P_{\max}$). The rest of the parameters could be deduced from the mathematical model equations and the PV technology [12,38].

2.2. SR-20 PV device modeling

In our practical platform, we have used an SR-20 PV device, with the specifications in the Table. According to the nonlinear algebraic equation (2), the implementation of the model is not obvious. To do so, we have used the Newton–Raphson numerical method [39]. The model has been implemented as a MATLAB C-S function in order to be compiled and loaded onto a dSpace board. The simulated $I--V$ and $P--V$ characteristics at nominal conditions are shown in Figure 2. The implemented model is able to reproduce the values of the key parameters of the PV device, such as V_{oc}, I_{scr}, V_{mp}, I_{mp}, and $P_{\max}$. The model was also validated with actual data on our practical platform. The irradiance, temperature, and voltage of the panel were measured and stored in a data file to be used as model inputs.

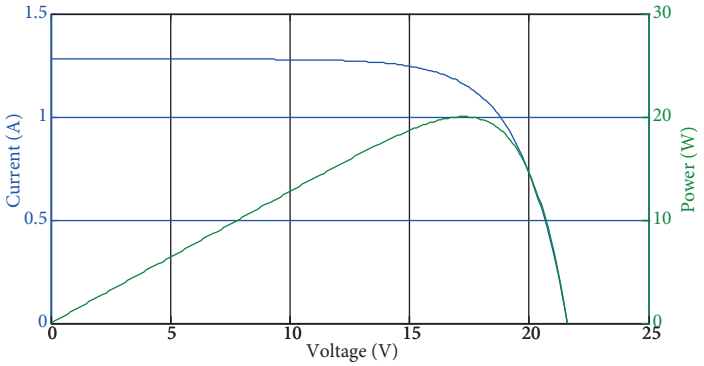

Figure 2. $I--V$ and $P--V$ characteristics of PV device at 1000 W/m^2, $T = 25\ ^\circ$ C.

The model was tested under natural conditions during short cloudy periods. The reproduced current by the established model of the SR-20 PV device follows with a good accuracy the measured current of the panel, as shown in Figure 3.

3. Proposed approach and simulation results

3.1. Principle

According to Eqs. (2), (3), and (4), which represent the $I--V$ characteristic of the panel, for a given value of T, G, and V, there is no more than one solution for the current I. The only value of the current could then

be computed by the model. Therefore, as the current is very sensitive to the irradiance level, the principle of the proposed method is to force the model to reproduce the same current as the one measured on the reference PV device, for given values of T, G, and V. Then the model has T, G, and V as inputs and the estimated current as output. The temperature is a very influential factor on the estimator. It should be measured and introduced in the model. Using the measured values for V and T inputs, the G input is computed by a PI controller in such way that the estimated current follows exactly the measured current's reference PV, as shown in Figure 4.

Table. SR-20 PV specifications (A.M.1.5, 1 kW/m^2, 25 $^\circ$ C), and parameters of the adjusted model at nominal operating conditions

Voltage at MPP	$V_{mp} = 17.2$ V	Band gap energy	$E_g = 1.12$ eV
Current at MPP	$I_{mp} = 1.17$ A	Reverse saturation current at T_r	$I_o = 5.98\text{e}^{-6}$ A
Short circuit current	$I_{scr} = 1.28$ A	Short circuit current generated at T_r	$I_{scr} = 1.28$ A
Open circuit voltage	$V_{oc} = 21.6$ V	Temperature coefficient of short circuit current	$k_i = 512.10^{-6}$ A/K
Maximum power	$P_{\max} = 20$ W	Number of cells connected in series	$n_s = 36$
Ideality factor	$A = 1.9$	Number of cells connected in parallel	$n_p = 1$
Charge of electron	$q = 1.6\text{e}^{-19}$C	Internal series resistance of a cell	$R_s = 0.004\ \Omega$
Boltzmann constant	$k = 1.38\text{e}^{-23}$ J/K	Internal parallel resistance of a cell	$R_p = 1000\ \Omega$

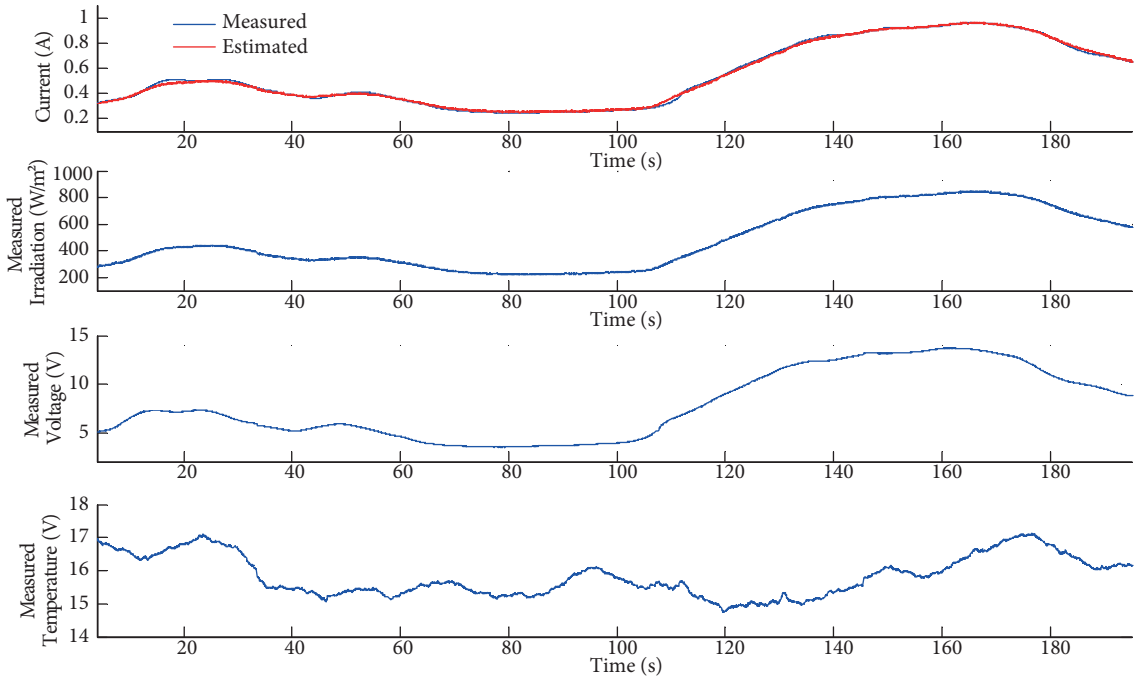

Figure 3. Model validation under natural conditions.

A PI controller is the proportional-integral part of the well-known proportional-integral-derivative controller (PID) in automatic control, [40]. It is widely used in control loop feedback mechanisms to bring a controlled process variable (output) to a desired setpoint.

The controller achieves this objective by using a manipulated variable (input), also called control variable, to minimize the error between the controlled variable and a desired setpoint. In our system, the control variable is the estimated irradiation G_{est}, while the controlled variable is the computed current I_{est} from the PV model.

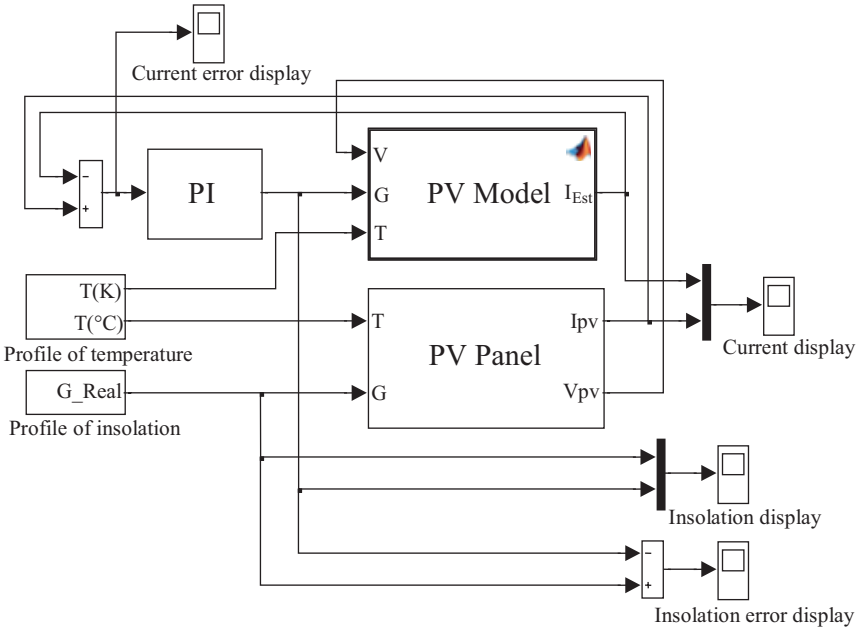

Figure 4. Simulation diagram of the proposed irradiation estimator.

The desired setpoint is the measured PV current I_{pv}. The control error to minimize is given by the equation

$$e(t) = I_{pv} - I_{est} \tag{5}$$

As its name suggests, the PI controller is based on two separate components, proportional and integral. The control variable is the sum of the contributions of both terms. The proportional contribution depends proportionally on the instantaneous value of the control error. It can be adjusted by multiplying the error by a constant K_p, called the proportional gain constant. The integral contribution is proportional to the accumulated error over time. It can be adjusted by multiplying the accumulated error by the integral gain K_{int}.

The mathematical equation of the PI controller is given by the following equation:

$$G_{est}(t) = \underbrace{K_p e(t)}_{\text{proportional term}} + \underbrace{K_{int} \int_0^t e(\tau) d\tau}_{\text{integral term}} \tag{6}$$

The closed loop used in the irradiation estimator is illustrated in Figure 5.

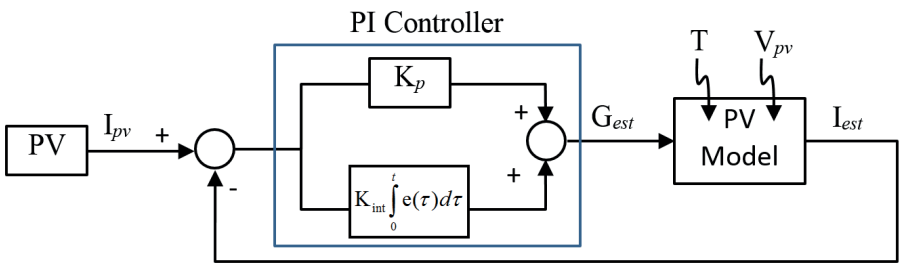

Figure 5. Diagram of the closed loop used in irradiation estimator.

The parameters K_p and K_{int} should be tuned to obtain the desired control performances. Several empirical and theoretical methods to adjust the PI parameters are found in the literature [40]. For our application, the performance needed is to ensure a fast convergence of the error towards zero. This can be achieved with sufficiently high gains. Indeed, high values of K_p ensure a fast response and high values of K_{int} ensure accuracy. A manual way to adjust these parameters is to initialize them to zero and then increment their values gradually to obtain fast and accurate convergence.

The PI controller algorithm could be implemented on a microprocessor for example.

3.2. Simulation results

In order to evaluate the performance of the estimator in various operating conditions, different levels of irradiation and temperature are used. Simulation tests were performed by MATLAB/Simulink. The simulation results for abrupt irradiation variations are shown in Figure 6. In this case, the estimated irradiation follows with a good accuracy the real value. The maximum irradiation error is less than 10 W/m^2. The results of the tests under natural conditions are shown in Figure 7.

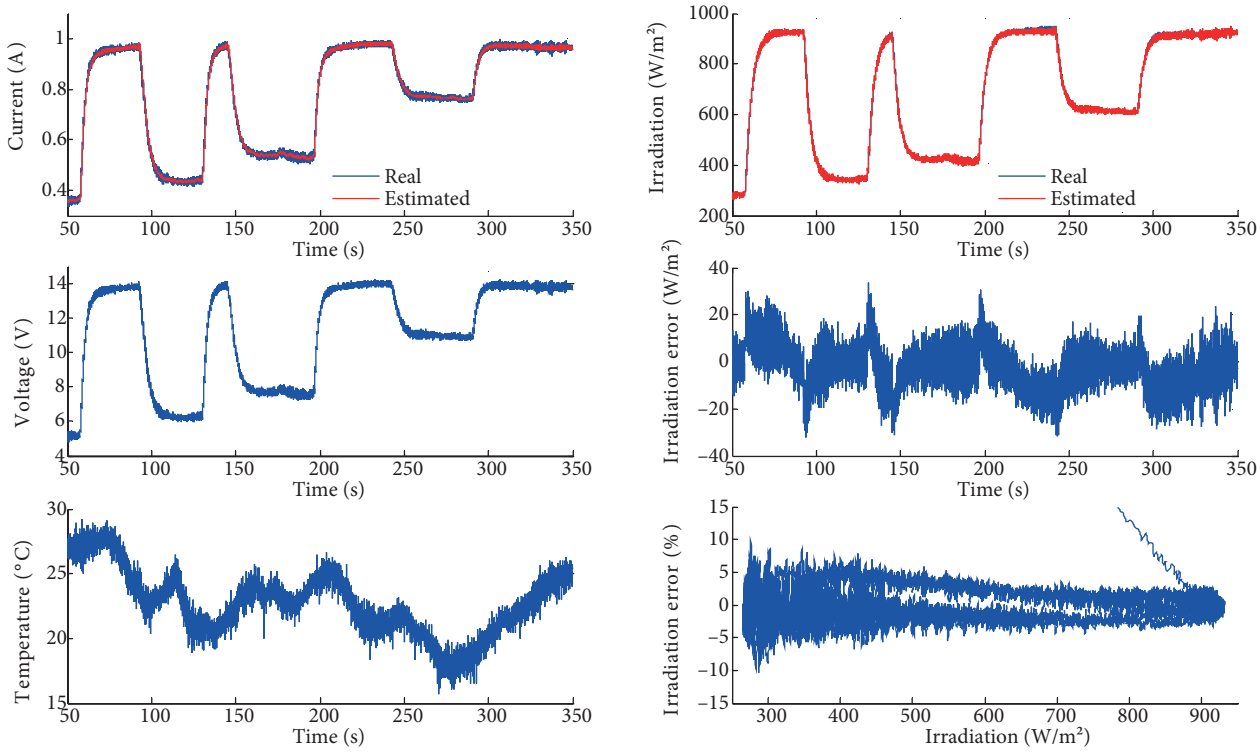

Figure 6. Simulation results with artificial variation in sunshine.

4. Experimental setup and results

An experimental device was designed to validate in real time the ability of our estimator to track the variation in the solar irradiance level. The sunshine variation was simulated using a mosquito screen with four layers, placed between the solar rays and the PV panel, including an irradiation sensor. Two kinds of mosquito screen, with close and wide mesh, were used. The screen effect of each layer reduces the irradiance level of approximately 150

W/m^2. Short cloudy periods also allowed us to test the estimator under natural conditions. The experimental setup and the real-time results are presented in the following subsections.

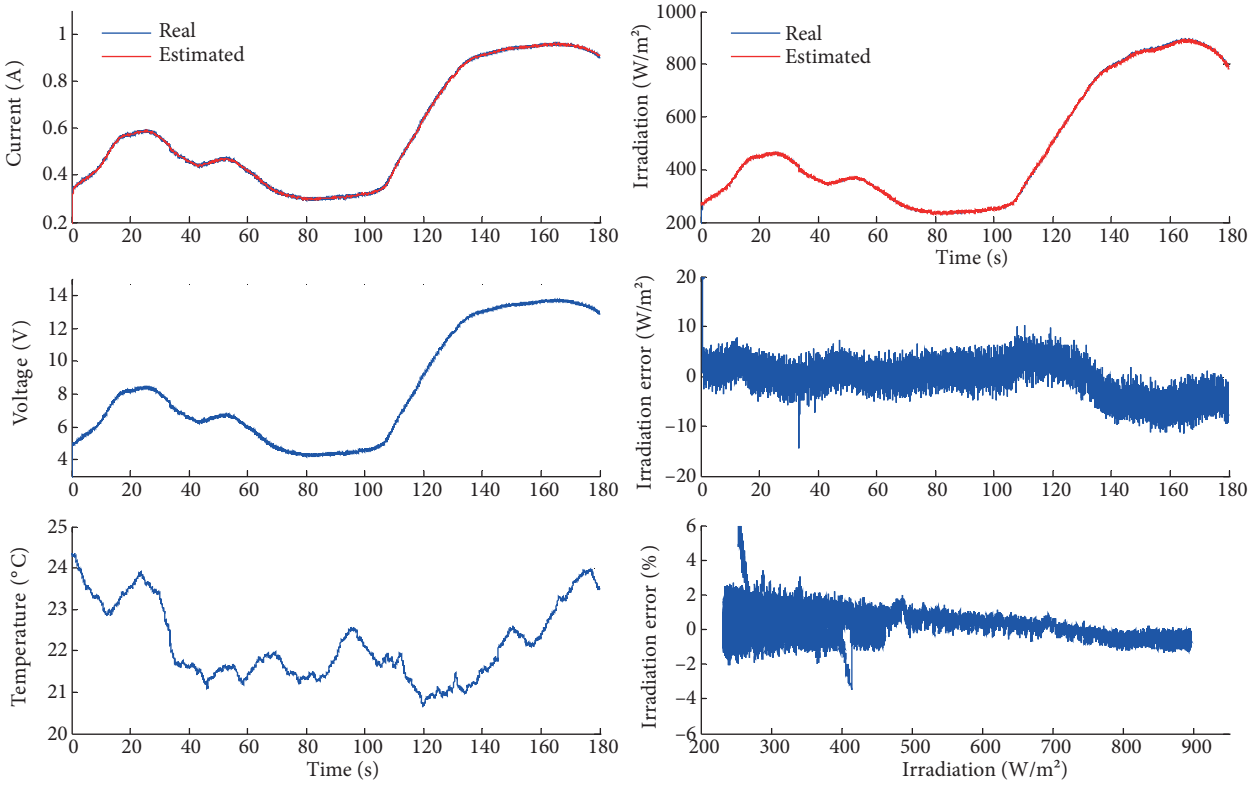

Figure 7. Simulation results in natural conditions.

4.1. Experimental setup

The proposed study has been implemented using a dSpace 1104 board, which works with MATLAB/Simulink software. Figure 8 is a schematic representation of the experimental platform. It consists of a PV module SR-20 connected to a resistive variable load.

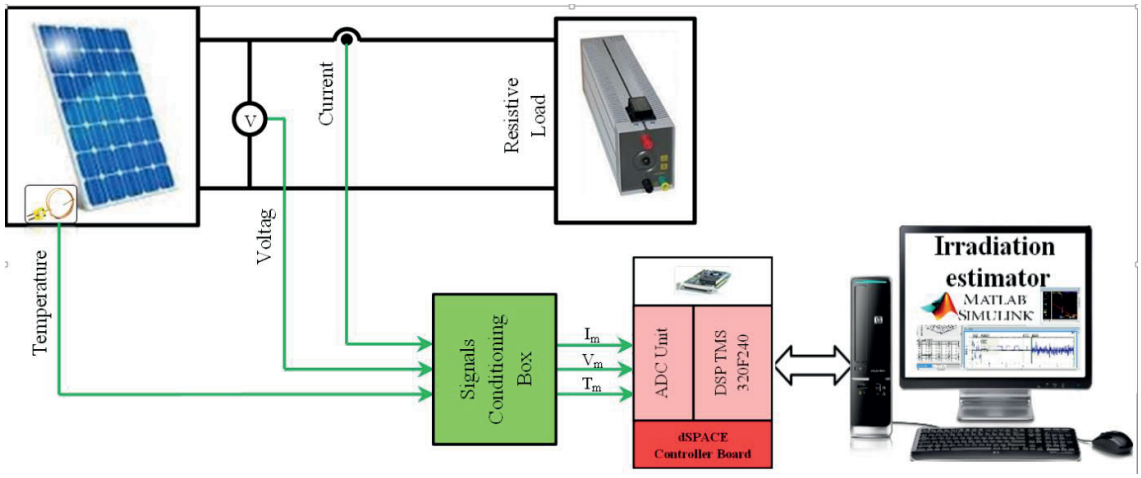

Figure 8. Experimental platform.

An LEM LA55-P current sensor, LEM LV20-P voltage sensor, and thermocouple temperature sensor (K) are used to measure respectively the current, voltage, and temperature of the PV module. All measured signals are conditioned and transformed in the voltage range 0 to ± 10 V and sent to the dSpace controller board. This includes an analogue–digital converter (ADC), a digital–analogue converter (DAC), and a processing system. The dSpace works on the MATLAB/Simulink platform, which is common engineering software. The dSpace boards are associated with Control Desk software, which makes the data acquisition and real-time analysis easy. The dSpace Real-Time Interface (RTI) is based on the MATLAB Real-Time Workshop (RTW) to create real-time codes.

The estimator algorithm consists of computing the closed loop, which is formed by the PV model and the PI controller. The algorithm has as inputs the current, voltage, and temperature of the PV module and has the estimated irradiation as output. The closed loop is carried out by a Simulink program. The Simulink box of the PV model is based on a C-S function code that allows a real-time compilation. The real-time code is loaded on the dSpace board. Real-time handling of data becomes then easily accessible via the Control Desk software. During the experimental validation, the noisy measured signals are eliminated using a low-pass filter.

The resistive load R_L could have any finite and nonzero value. However, since the principle of the estimator is based on the current as the controlled variable, it is judicious to work around an operating point at which the panel can be considered as a current source. Figure 9 shows that by choosing $R_L = R_{mp} = V_{mp}/I_{mp} = 14.7\ \Omega$, the panel is at its optimal operating point under standard conditions (1000 W/m^2 and 25 ° C). Note that V_{mp} and I_{mp} are given in the data sheet of the panel. Thus, when the irradiation level decreases for example to 600 W/m^2 and 200 W/m^2 , the operating point goes back toward the zone where the panel behaves as a current source. In Figure 9, the points Op1, Op2, and Op3 correspond respectively to the operating point positions for irradiation values 1000 W/m^2, 600 W/m^2, and 200 W/m^2.

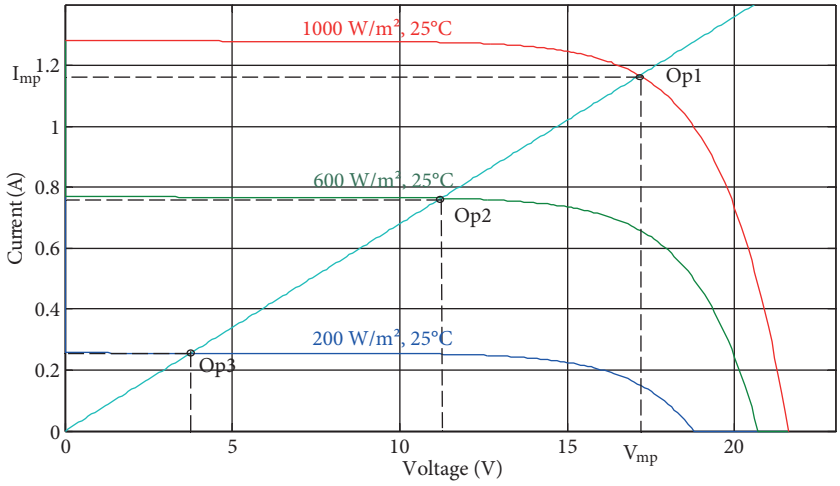

Figure 9. Variation of PV operating point according to the irradiation level.

As can be observed in Figure 10, the temperature has no significant influence on the operating point value, especially for irradiations lower than 1000 W/m^2.

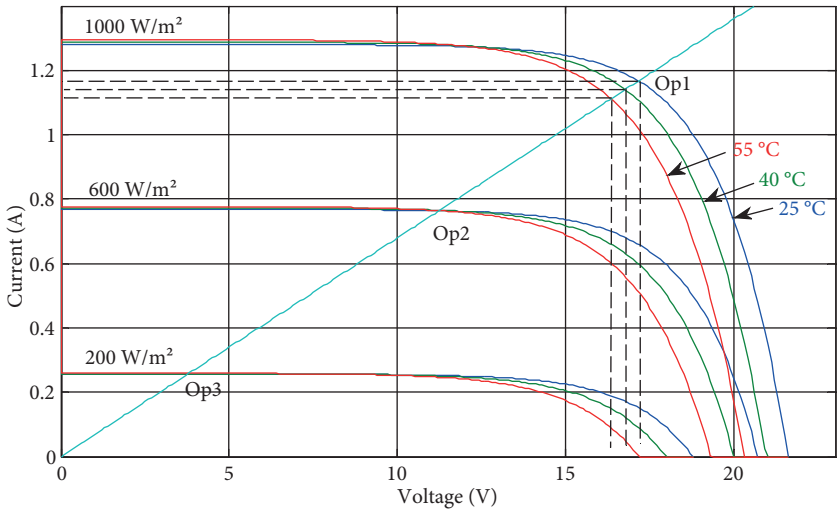

Figure 10. Effect of the temperature on the PV operating point.

4.2. Experimental results

4.2.1. Controlled irradiance variation

The experimental results obtained with artificial progressive variation in sunshine and the control loop performance are illustrated in Figure 11. A validation test was performed in Marrakech on 27 November 2013

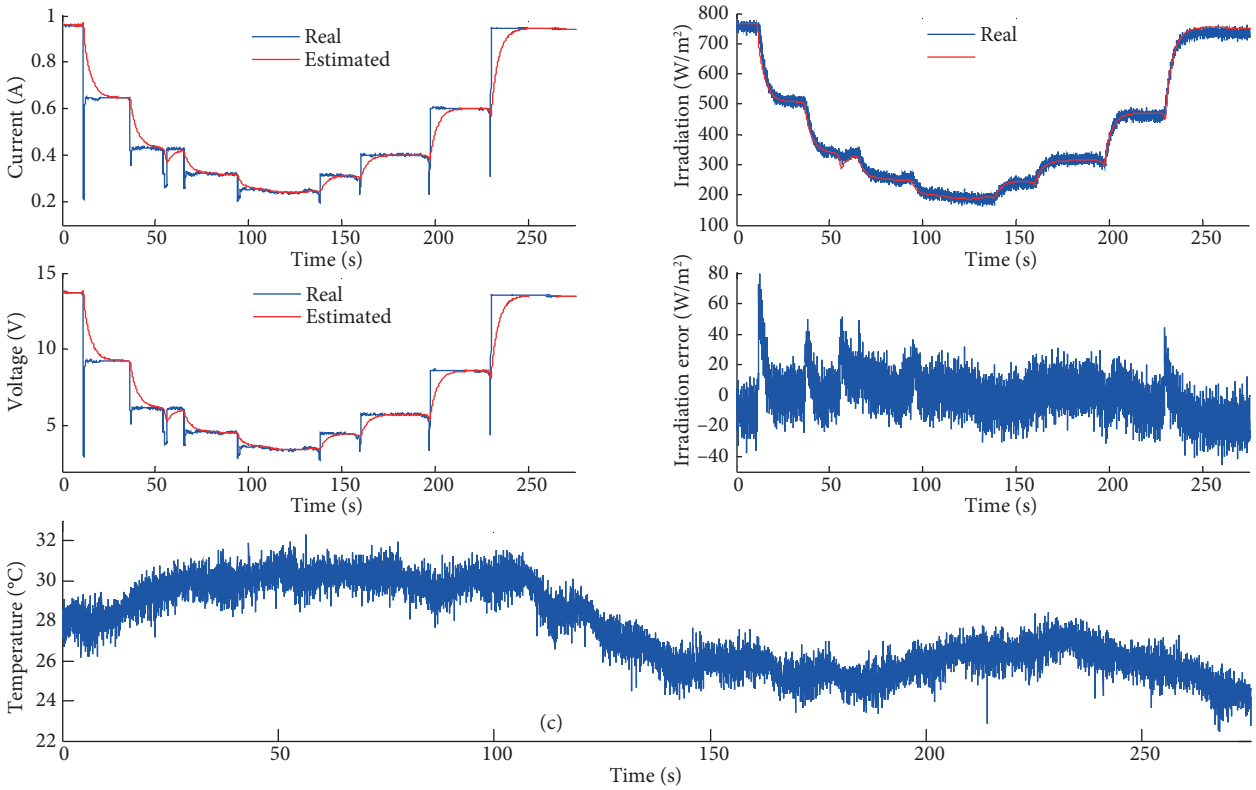

Figure 11. Experimental results with artificial progressive variation in sunshine.

at 1530. The decrease and increase in irradiation level were performed by adding and removing gradually the four layers of the mosquito screen. The controlled current of the model tracks well the measured current. The maximum error of estimation is observed during transients. It could be improved with a good tuning of the PI controller parameters. As can be expected, the estimated voltage has the same behavior as the measured one after transients. The results show that our estimator is able to accurately track changes in the irradiation. The maximum measured power is 755 W/m^2. As can be observed, the use of the four layers together could reduce the sunlight intensity to very low levels, namely 185 W/m^2 in the present experiment. Good accuracy was also obtained under high irradiance variations as shown in Figure 12.

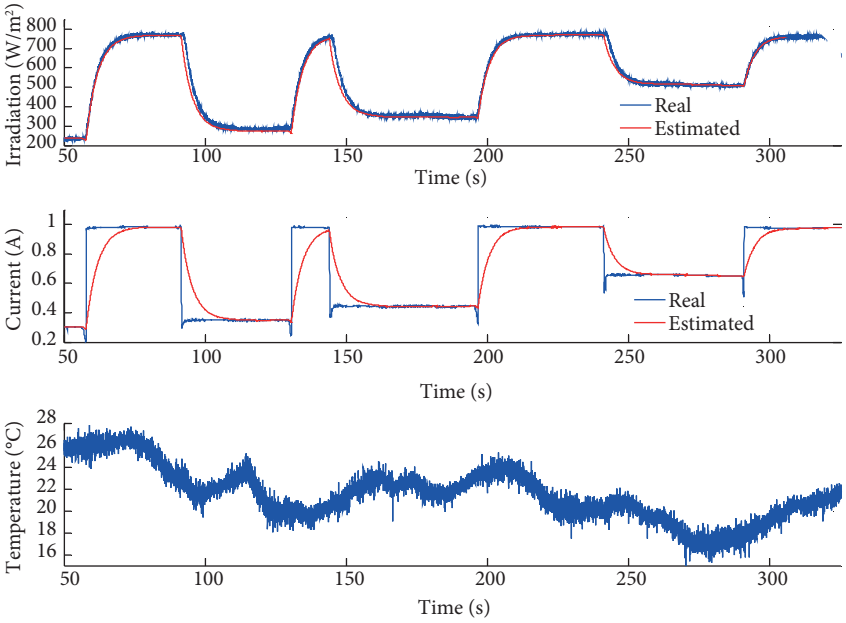

Figure 12. Experimental results with artificial abrupt variations in sunshine.

4.2.2. Natural irradiance variation

Tests under natural conditions, during cloudy periods, were carried out in Marrakech on 10 December 2013 at 1200 as shown in Figure 13. In these tests, the sunshine level varies between 500 W/m^2 and 1000 W/m^2. The results show good performance of the estimator.

5. Error analysis

To determine the accuracy of the proposed method, the so-called irradiation error in the paper should be analyzed. We define the irradiation error as the difference between the irradiation value determined by our estimator and the reference irradiation measured by the pyranometer CM10, Eq. (7).

$$Irr\_err(W/m^2) = (G_{mes} - G_{est}) \tag{7}$$

The relative error is defined as the percentage (%) of the previously defined error compared to the reference irradiation, Eq. (8).

$$Irr\_err\_rel(\%) = 100\frac{|Irr\_err|}{G_{mes}} \tag{8}$$

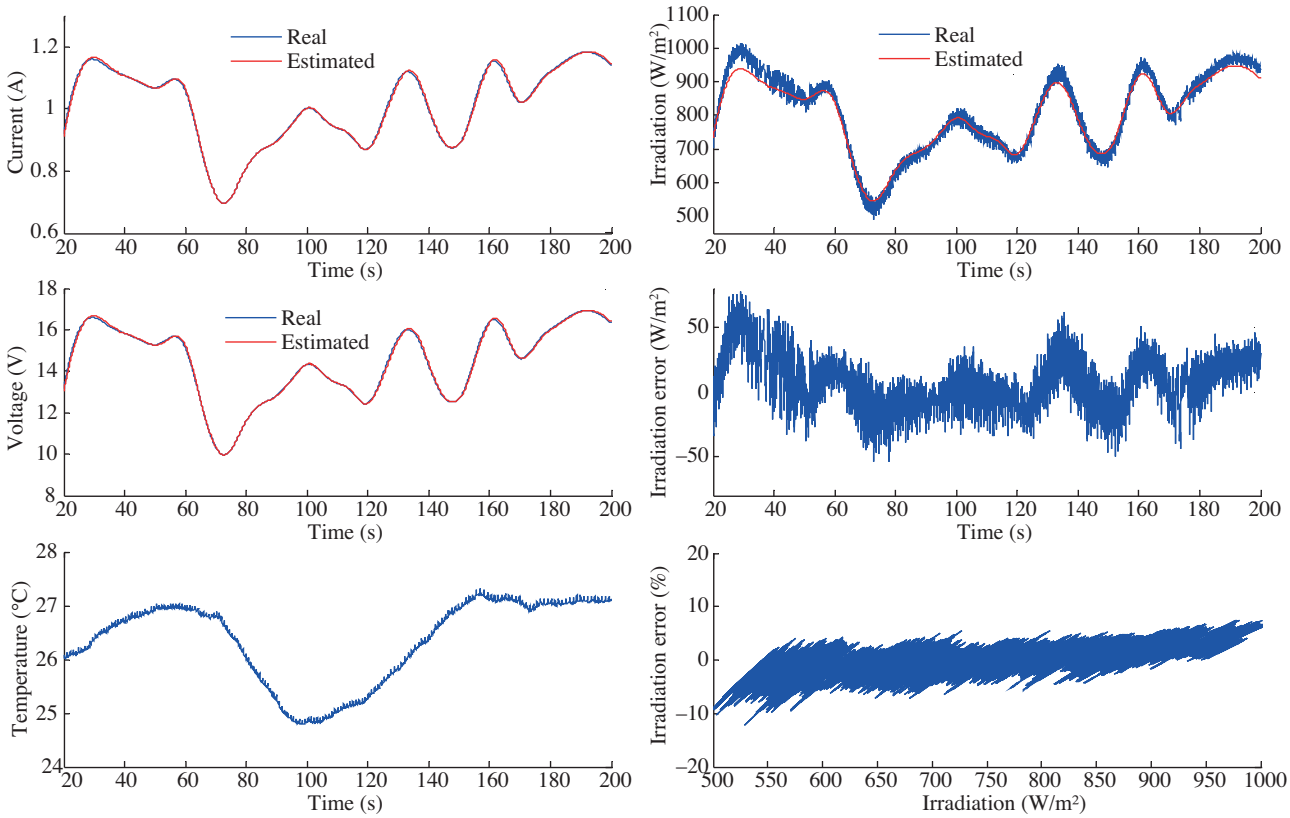

Figure 13. Experimental results in natural conditions.

This error could be potentially influenced by several factors. The first factor is related to the accuracy of the reference irradiation sensor used to validate the method. According to its data sheet, the sensor is characterized by a maximum error of 1%. A second potential source of error could be the instrumentation of our platform. A third potential error source is related to our algorithm. In this case, two elements should be considered: the accuracy of the identified PV model and the fastness of the estimator closed loop. Concerning the model, its validation showed high accuracy, as shown in Figure 3. Finally the fastness of the estimator convergence can be ensured by choosing sufficiently high PI controller gains.

5.1. Error of simulation results

By analyzing the simulation results shown in Figures 6 and 7, the maximum relative error is respectively less than 5% and 2%. The maximum relative error decreases for higher radiation levels. The error in the first case is a little larger than that in the second case because of the abrupt artificial changes in the irradiation level that are faster than the closed-loop response.

5.2. Error of experimental results

The conclusions of simulation results remain the same in the real-time tests presented in Figures 11, 12, and 13. However, the maximum relative error, which is about 4% under natural conditions, is slightly larger than 2% generated in simulation. This is typically due to the acquisition system and the platform instrumentation. This error could be reduced in the final prototype by eliminating all sources of noise.

6. Conclusion

In this paper, we have introduced a new approach to estimate local solar irradiation, based on a mathematical model of a PV cell and a PI controller. The measured temperature, the PV current, and the voltage should be used as inputs of the estimator. The effectiveness of the estimator was proved in simulation and in practice under realistic conditions. The obtained results show that the estimated irradiation tracks the sunlight level variations as fast as they are with a minimal estimation error. The maximum measured irradiation error is less than 4% relative to the measured sunshine. This error could be reduced in the final prototype by eliminating all sources of noise, including cables and the acquisition system.

Some prospects for this application are considered. A prototype of the solar irradiation sensor will be designed with a solar cell and implemented on a microcontroller and will be validated with a very accurate standard sensor. The use of the principle of the method in PV performance analysis under partial sunshine could be studied. The application to sensorless solar trackers is under study and seems to be very promising. The detection of failures in solar installations could also be considered.

References

[1] Parida B, Iniyan S, Goic R. A review of solar photovoltaic technologies. Renew Sust Energ Rev 2011; 15: 1625-1636.

[2] Goetzberger A, Hoffmann VU. Photovoltaic Solar Energy Generation. 1st ed. Berlin, Heidelberg, Germany: Springer Series in Optical Sciences, 2005.

[3] Schaefer JC. Review of photovoltaic power plant performance and economics. IEEE T Energy Conver 1990; 5: 232-283.

[4] Kininger F. Photovoltaic systems technology. Kassel, Germany: Universität Kassel, Institut für Rationelle Energiewandlung, 2003.

[5] Tsai HL. Insolation-oriented model of photovoltaic module using Matlab/Simulink. Sol Energy 2010; 84: 1318-1326.

[6] Esram T, Chapman PL. Comparison of photovoltaic array maximum power point tracking techniques. IEEE T Energy Conver 2007; 22: 439-449.

[7] Ishaque K, Salam Z. A review of maximum power point tracking techniques of PV system for uniform insolation and partial shading condition. Renew Sustain Energ Rev 2013; 19: 475-488.

[8] Sera D, Teodorescu R, Jochen H, Knoll M. Optimized maximum power point tracker for fast-changing environmental conditions. IEEE T Ind Electron 2008; 55: 2629-2637.

[9] Kulaksiz AA. ANFIS-based estimation of PV module equivalent parameters: Application to a stand-alone PV system with MPPT controller. Turk J Electr Eng & Comp Sci 2013; 21: 2127-2140.

[10] Riordan C, Hulstron R. What is an air mass 1.5 spectrum? [Solar cell performance calculations]. In: IEEE 1990 Photovoltaic Specialists Conference; 21–25 May 1990; Kissimmee, FL, USA: IEEE. pp. 1085-1088.

[11] ASTM G173-03 Standard tables for Reference Solar Spectral Irradiances: Direct Normal and Hemispherical on 37 Tilted Surface.

[12] Villalva MG, Gazoli JR, Filho ER. Comprehensive approach to modeling and simulation of photovoltaic arrays. IEEE T Power Electr 2009; 24: 1198-1208.

[13] Xiao W, Dunford WG, Capel A. A novel modeling method for photovoltaic cells. In: IEEE 2004 Power Electronics Specialists Conference; 20–25 June 2004; Vancouver, BC, Canada: IEEE. pp. 1950-1956.

[14] Angstrom AK. Solar and terrestrial radiation. Q J Roy Meteor Soc 1924; 50: 121-126.

[15] Liu BYH, Jordan RC. The interrelationship and characteristic distribution of direct, diffuse and total solar radiation. Sol Energy 1960; 4: 1-19.

[16] Swartman RK, Ogunlade O. Solar radiation estimates from common parameters. Sol Energy 1967; 11: 170-172.

[17] Collares-Pereira M, Rabl A. The average distribution of solar radiation-correlations between diffuse and hemispherical and between daily and hourly insolation values. Sol Energy 1979; 22: 155-164.

[18] Brock TD. Calculating solar radiation for ecological studies. Ecol Model 1981; 14: 1-19.

[19] Duffie JA, Beckman WA. Solar Engineering of Thermal Processes. 4th ed. New York, NY, USA: Wiley, 2013.

[20] Gopinathan KK. A simple method for predicting global solar radiation on a horizontal surface. Sol Wind Tech 1988; 5: 581-583.

[21] Husain NS, Zainal NA, Singh BSM, Mohamed NM, Mohd Nor N. Integrated PV based solar insolation measurement and performance monitoring system. In: IEEE 2011 Humanities Science and Engineering Research Colloquium; 5–6 December 2011; Penang, Malaysia: IEEE. pp. 710-715.

[22] Gallego AJ, Camacho EF. Estimation of effective solar irradiation using an unscented Kalman filter in a parabolic-trough field. Sol Energy 2012; 86: 3512-3518.

[23] Yu B, Abo-KhaliI AG, So J, Yu G. Support vector regression based maximum power point tracking for PV grid-connected system. In: IEEE 2009 Photovoltaic Specialists Conference; 7–12 June 2009; Philadelphia, PA, USA: IEEE. pp. 2037-2042.

[24] Dunn L, Gostein M, Emery K. Comparison of pyranometers vs. PV reference cells for evaluation of PV array performance. In: IEEE 2012 Photovoltaic Specialists Conference; 3–8 June 2012; Austin, TX, USA: IEEE. pp. 2899-2904.

[25] Aziz FSA, Sulaiman SI, Zainuddin H. A prototype of an integrated pyranometer for measuring multi-parameters. In: IEEE 2013 Signal Processing and its Applications International Colloquium; 8–10 March 2013; Kuala Lumpur, Malaysia: IEEE. pp. 73-77.

[26] Driesse A, Dirnberger D, Reise C, Reich N. Spectrally selective sensors for PV system performance monitoring. In: IEEE 2012 Photovoltaic Specialists Conference; 3–8 June 2012; Austin, TX, USA: IEEE. pp. 3294-3299.

[27] Donovan M, Bourne B, Roche J. Efficiency vs. irradiance characterization of PV modules requires angle-of-incidence and spectral corrections. In: IEEE 2010 Photovoltaic Specialists Conference; 20–25 June 2010; Honolulu, HI, USA: IEEE. pp. 2301-2305.

[28] Spertino F, Di Leo P, Cocina V. Accurate measurements of solar irradiance for evaluation of photovoltaic power profiles. In: IEEE 2013 Power Tech; 16–20 June 2013; Grenoble, France: IEEE. pp. 1-5.

[29] Phang JCH, Chan DSH, Philips JR. Accurate analytical method for the extraction of solar cell model parameters. Electron Lett 1984; 20: 406-408.

[30] Angrist SW. Direct Energy Conversion. 4th ed. Boston, MA, USA: Allyn and Bacon, 1982.

[31] Fritz S. Solar energy on clear and cloudy days. Sci Monthly 1957; 84: 55-56.

[32] Rauschenbach HS. Solar Cell Array Design Handbook - The Principles and Technology of Photovoltaic Energy Conversion. 1st ed. New York, NY, USA: Van Nostrand Reinhold Co, 1980.

[33] Lo Brano V, Orioli A, Ciulla G, Di Gangi A. An improved five-parameter model for photovoltaic modules. Sol Energ Mat Sol C 2010; 94: 1358-1370.

[34] Celik AN, Acikgoz N. Modelling and experimental verification of the operating current of mono-crystalline photovoltaic modules using four- and five-parameter models. Appl Energy 2007; 84: 1-15.

[35] Shen W, Ding Yi, Choo FH, Wang P, Loh PCh, Tan KK. Mathematical model of a solar module for energy yield simulation in photovoltaic systems. In: IEEE 2009 Power Electronics and Drive Systems International Conference; 2–5 November 2009; Taipei, Taiwan: IEEE. pp. 336-341.

[36] De Soto W, Klein SA, Beckman WA. Improvement and validation of a model for photovoltaic array performance. Sol Energy 2006; 80: 78-88.

[37] Kou Q, Klein SA, Beckman WA. A method for estimating the long-term performance of direct-coupled PV pumping systems. Sol Energy 1998; 64: 33-40.

[38] Tsai HL, Tu CS, Su YJ. Development of Generalized Photovoltaic Model Using MATLAB/SIMULINK. In: Proceedings of the World Congress on Engineering and Computer Science; 22–24 October 2008; San Francisco, CA, USA: WCECS. pp. 846-851.

[39] Chapra SC, Canale RP. Numerical Methods for Engineers, 6th ed. New York, NY, USA: McGraw-Hill, 2009.

[40] Åström KJ, Hägglund T. PID controllers: Theory, design and tuning. Instrumentation Society of America: Research Triangle Park, 1995.